J Mater Sci: Mater Med (2010) 21:2623–2635
DOI 10.1007/s10856-010-4111-8

In vitro degradation behavior and cytocompatibility of Mg–Zn–Zr alloys

Z. G. Huan · M. A. Leeflang · J. Zhou · L. E. Fratila-Apachitei · J. Duszczyk

Received: 6 November 2009 / Accepted: 25 May 2010 / Published online: 9 June 2010

Abstract Zinc and zirconium were selected as the alloying elements in biodegradable magnesium alloys, considering their strengthening effect and good biocompatibility. The degradation rate, hydrogen evolution, ion release, surface layer and in vitro cytotoxicity of two Mg–Zn–Zr alloys, i.e. ZK30 and ZK60, and a WE-type alloy (Mg–Y–RE–Zr) were investigated by means of long-term static immersion testing in Hank's solution, non-static immersion testing in Hank's solution and cell-material interaction analysis. It was found that, among these three magnesium alloys, ZK30 had the lowest degradation rate and the least hydrogen evolution. A magnesium calcium phosphate layer was formed on the surface of ZK30 sample during non-static immersion and its degradation caused minute changes in the ion concentrations and pH value of Hank's solution. In addition, the ZK30 alloy showed insignificant cytotoxicity against bone marrow stromal cells as compared with biocompatible hydroxyapatite (HA) and the WE-type alloy. After prolonged incubation for 7 days, a stimulatory effect on cell proliferation was observed. The results of the present study suggested that ZK30 could be a promising material for biodegradable orthopedic implants and worth further investigation to evaluate its in vitro and in vivo degradation behavior.

Z. G. Huan · M. A. Leeflang · J. Zhou (✉) · L. E. Fratila-Apachitei · J. Duszczyk
Department of Materials Science and Engineering, Delft University of Technology, Mekelweg 2, 2628 CD Delft, The Netherlands
e-mail: j.zhou@tudelft.nl

1 Introduction

In recent years, there has been growing interest in magnesium alloys as a new generation of biodegradable materials [1]. Biodegradable magnesium and its alloys are advantageous over existing biodegradable materials such as polymers, ceramics and bioactive glasses in load-bearing applications where sufficient strength and Young's modulus close to that of the bone are required [2]. However, fast degradation of magnesium due to corrosion in the human bio-environment may limit its clinical applications [1, 3], for example, orthopedic applications, because a too high degradation rate leads to premature deterioration of biofunctionality.

Alloying is a general approach to improving the corrosion resistance of magnesium as well as its mechanical properties. It is however restricted in the case of designing magnesium alloys for biomedical applications, when the toxicity of alloying elements is taken into consideration. Most of the magnesium alloys that have so far been investigated as potential implant materials are rather complex in alloy composition and contain potentially toxic alloying elements [1, 4]. Aluminum-containing magnesium alloys, for example, are not preferred material choices for biomedical applications, because accumulation of aluminum is associated with various neurological disorders [5]. As to the alloys containing rare earth mischmetal elements in addition to yttrium (e.g. WE43), controversy exists as to the biological effects of rare-earth elements in these alloys [6, 7]. In a clinical trial for acute treatment of a newborn with severely impaired heart function, for example, Mg-based absorbable stents containing rare-earth elements are reportedly not tolerated [8].

In principle, in the design and selection of a biodegradable metallic material, elements with potential toxicological problems should be avoided altogether or limited

to minimum acceptable amounts, if these elements cannot really be excluded from the alloy [9]. Another important issue, which is sometimes not addressed, concerns the composition and processing of the material. Both should not be too complex to make systematic in vivo evaluation as well as further alloy and processing optimization difficult. With the above considerations in mind, in the present research, zinc and zirconium were chosen as the alloying elements in biodegradable magnesium alloys for biomedical applications. Zinc (Zn) is a common alloying ingredient in magnesium and its strengthening effect is second only to aluminum. It helps overcome the harmful corrosive effect of impurities such as iron and nickel, thus improving the corrosion resistance of magnesium alloys [10, 11]. Its concentration is usually limited to 3% for good corrosion resistance [12, 13]. In addition, zinc is considered an essential micro-nutrient, as zinc-deficiency may result in strongly perturbed physiological functions in the human body [14]. Zirconium (Zr) is usually used as a grain refiner in magnesium alloys without aluminum, thereby contributing to the strength of these alloys [15]. It also reduces the adverse effect of iron contaminant on the corrosion resistance of magnesium alloys [16]. In the Mg–Zr binary alloy system, zirconium is effective in enhancing corrosion resistance only when its content is less than 0.48% with no Zr-containing precipitates forming [17]. While the importance of zirconium in the human body is still being determined, it has been reported that zirconium shows both in vitro and in vivo good biocompatibility and osseointegration, even outperforming titanium [18, 19].

Up till now, limited research has been carried out on Mg–Zn–Zr alloys as potential biodegradable materials, although an addition of zinc to magnesium was recognized as a good direction to take [3]. Notwithstanding this, it has been confirmed that the Mg–6Zn–0.6Zr alloy (ZK60) in simulated body fluid degrades faster than pure magnesium [13]. Therefore, a leaner magnesium alloy with 3% Zn and 0.6% Zr (ZK30) was selected for the present research. To authors' best knowledge, no preceding research had been carried out on this alloy for biomedical applications. As can be seen from Table 1, with the same Zr content, ZK30 mechanically underperforms ZK60 only to a limited extent.

In the present study, in vitro degradability of ZK30 was evaluated with respect to mass loss and hydrogen evolution during long-term static immersion tests. Its degradation behavior was further investigated in terms of ion release and pH value of non-static Hank's solution over a period of 7 days. Its cytocompatibility was evaluated by testing cell viability in vitro under the influence of the eluate of the material [7, 20]. Comparison was made with a WE-type alloy as well as with hydroxyapatite (HA) in order to establish the viability of the ZK30 alloy as a potential biodegradable material for biomedical applications. The rationale behind choosing a WE-type alloy for comparison purposes was that the WE43 alloy was previously investigated in vitro and in vivo as a potential material for orthopedic applications and it showed good corrosion resistance and cytocompatibility, relative to other magnesium alloys (AZ31, AZ91 and LAE42) [6]. Its typical tensile properties in comparison with those of ZK30 and ZK60 are given in Table 1.

2 Materials and experimental details

2.1 Material preparation

ZK60 and ZK30 alloys were prepared from high-purity Mg (>99.95%), Zn (>99.9%) and Mg–30Zr (wt%) master alloy. A WE-type alloy was prepared from high purity-Mg (>99.95), pure yttrium, pure neodymium and gadolinium (Nd:Gd = 80:20, instead of Nd-rich rare earths), as well as Mg–30Zr master alloy. The raw materials were melted in an electric-resistance furnace under gas flux protection. After a grain-refining procedure at 760–800°C, the melt was poured into a steel mould preheated to 200–300°C. After solidification, rods were cut from the ingots and a surface layer was machined off. The rods were cut into disks with a diameter of 28 mm and a thickness of 5 mm without further polishing. The exact chemical compositions of the ZK30, ZK60 and WE-type alloy disks determined using an X-ray fluorescence spectrometer (Phillips PW-4200) are given in Table 2.

2.2 Static immersion tests to determine degradation rate and hydrogen evolution

While the conventional corrosion testing techniques, such as potentiometric testing, are of great value for the

Table 1 Typical mechanical properties of the ZK30, ZK60 and WE43 alloys [2]

Alloy	Nominal composition	0.2% proof strength (MPa)	Ultimate tensile strength (MPa)	Elongation at fracture (%)
ZK30	Mg–3Zn–0.6Zr	215	300	9
ZK60	Mg–6Zn–0.6Zr	235	315	8
WE-43	Mg–4Y–3RE[a]–0.5Zr	160	260	6

[a] RE consists of 2.0–2.5% neodymium, the remainder being heavy rare earths, principally ytterbium, erbium, dysprosium and gadolinium

Table 2 Chemical compositions of the magnesium alloys under investigation (wt%)

Alloys	Zn	Zr	Fe	Cu	Ni	Y	RE[a]	Mg
ZK30	3.15	0.43	0.007	–[b]	–	–	–	Bal.
ZK60	5.86	0.42	–	–	–	–	–	Bal.
WE-type	0.006	0.42	0.011	–	–	5.00	3.61	Bal.

[a] RE consists of Nd and Gd at a ratio of Nd:Gd = 80:20

[b] Indicates that the concentration is lower than 50 mg/kg

assessment of the potential of an alloy to corrode, they do not provide information specific to the possibility of the alloy to be considered as a degradable biomaterial [21]. Therefore, instead of electrochemical testing, long-term static immersion tests in Hank's solution, together with the measurement of hydrogen evolution [13], were performed to investigate the degradation behavior of the alloys over a period of 21 weeks. A burette filled with the solution was placed over the sample in a beaker filled with the same solution in order to collect the hydrogen evolving during the degradation tests. The tests were performed at 37.0°C in a thermostatic bath. Hank's solution was selected, because it represented the ion concentrations of blood plasma [22]. The ion concentrations of Hank's solution in comparison with those of human blood are presented in Table 3 [23]. As can be seen, the Cl^- ion concentration in Hank's solution is actually higher than that in human blood, thus presenting a highly hostile condition for magnesium alloys. For each disk-shaped sample, 250 ml of Hank's solution was used. During the testing over 21 weeks, the whole immersion system was regularly refilled with deionized water to a level of 250 ml in order to compensate for the liquid loss due to evaporation in the ambient atmosphere. Mass loss was registered once a week and the hydrogen evolution was monitored on a daily basis.

2.3 Non-static immersion tests to analyze ion release and characterize surface layer

To investigate the behavior of ion release in greater detail and characterize the surface layer at the early stage of degradation, samples in the form of disks with a diameter of 10 mm, a thickness of 2 mm and thus a surface-area-to-volume ratio of 0.1 cm^{-1} were prepared and immersed in Hank's solution at 37.0°C [24]. A shaker incubator was used and agitation was maintained at 30 rpm. To determine the influence of a compositional change of Hank's solution on the in vitro behavior of the alloys, after 24 h immersion, one half of the volume of the soaking medium was collected for further investigation and the rest refreshed with new Hank's solution. An inductively coupled plasma optical emission spectrometer (ICP-OES, PerkinElmer Optima 3000dv) was employed to determine the concentrations of magnesium and other metal ions dissolved from the disk samples. The changes in Ca and P ions were also registered. The pH value of the solution collected after 24 h immersion was measured using an electrolyte-type pH meter (pH-meter CG840, Den Bosch, Holland). The procedure was repeated every day throughout a period of 7 days. The initial ion concentrations and pH value of Hank's solution were taken as the starting points and used as the data of day zero.

After 1-day and 7-day non-static immersion as described above, samples were taken out of the soaking medium and gently rinsed with deionized water to remove retained soaking medium. Their surfaces were cleaned with ethanol, followed by drying at room temperature. To identify the compounds of the surface layer, an X-ray diffractometer (XRD, Bruker-AXS D5005) was used with 2-theta angles ranging from 10 to 80°. Diffraction spectra were interpreted qualitatively using the powder diffraction file (PDF). The surface morphology and the compositions of the compounds formed on the sample surfaces after non-static immersion were analyzed by using a scanning electron microscope (JSM-6500F, JEOL) equipped with an energy dispersive X-ray (EDX) spectrometer (INCA Energy, Oxford Instruments).

2.4 Cytotoxicity testing of degradation products

Rabbit bone marrow stromal cells (rBMSC) were isolated and expanded using an established method with minimum modifications [25]. Cytotoxicity tests were carried out by indirect contact. The cells were cultured in the extracts from the degrading material. Extracts were prepared using a RPMI 1640 (Gibco) cell culture medium as the extraction medium with an extracting medium volume to surface area ratio of 1.25 ml/cm^2 in a humidified atmosphere with 5%

Table 3 Ion concentrations in human blood and Hank's solution (mg/L)

	Na^+	K^+	Ca^{2+}	Mg^{2+}	Cl^-	HCO_3^-	HPO_4^{2-} and $H_2PO_4^-$
Blood plasma [23]	3266	156	100	24	3657	1708	246
Hank's solution[a]	3241	226	46	17	5135	254	75

[a] Data posted on the website www.sigmaaldrich.com and the elemental concentrations of Ca, Mg and P, measured by using ICP-OES, being 45.8, 16.9 and 21.8 mg/l, respectively

CO_2 at 37°C for 24 h [7]. The supernatant fluid was withdrawn and centrifuged to prepare the extraction culture medium.

Cell suspension was adjusted to a density of 1×10^4 cell/ml and 100 µl of cell suspension was added to each well of a 96-well plate and incubated for 24 h. The culture medium was then removed and replaced by 50 µl of extracts and 50 µl of RPMI 1640 medium supplemented with 20% fetal calf serum (FCS) every second day. The number of viable cells was quantitatively assessed by the MTT test [26]. MTT (Sigma) [3-(4,5-dimethylthiazol-2-yl)-2,5-diphenyl tetrazolium bromide] is a yellow tetrazolium salt that can be enzymatically converted by a living cell to a purple formazan product. The intensity of the color produced is therefore directly proportional to the number of viable cells in culture and thus to their proliferation in vitro. The absorbance of the color can be measured at 590 nm (A590). In the present tests, after incubating at 37°C and in an atmosphere with 5% CO_2 for one and 7 days [7, 27], 100 µl of the 0.5 mg/ml MTT solution was added to the well plate and incubated for 4 h at 37°C. Then 100 µl of dimethyl sulfoxide was added to each well and the plate was shaken for 5 min. The optical density (OD) at 590 nm was measured with an enzyme-linked immunoadsorbent assay plate reader (ELX800, Bio-TEK). A cytocompatible hydroxyapatite (HA) disk was used as reference [28, 29]. Six samples per group were tested in the experiment. The results were compared in OD units.

2.5 Statistical methods

The experimental values were analyzed using the Student's *t*-test and expressed by the mean values ± standard deviation (SD). A P-value < 0.05 was considered statistically significant.

3 Results

3.1 Mass loss and hydrogen evolution during static immersion

The mass loss of samples during the static immersion tests is shown in Fig. 1. It can be seen that ZK30 and WE-type alloy samples had quite similar degradation rates during the first 14 weeks of immersion. However, during prolonged immersion from 14 to 21 weeks, the degradation rate of WE-type alloy sample deviated slightly from that of ZK30 sample. It is remarkable that the mass loss of the ZK30 sample in the immersion tests for 21 weeks was still minute, while ZK60 showed an accelerated degradation rate in the first 9 weeks. At the end of week 12, ZK60 sample was completely degraded.

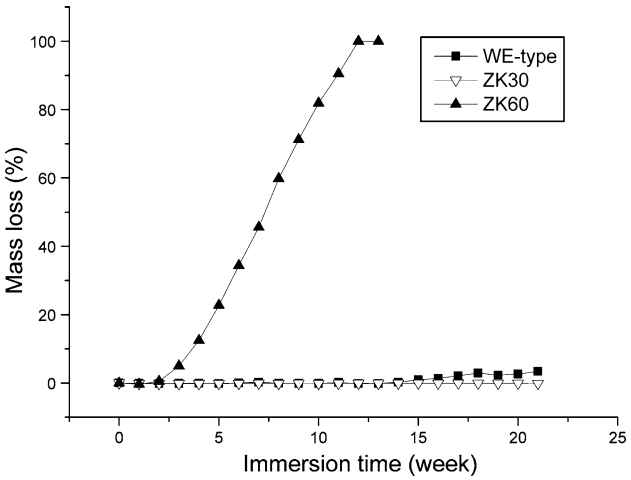

Fig. 1 Mass loss as a function of time during static immersion in Hank's solution

Surface macro-morphologies of some of the samples throughout 21-week static immersion tests are shown in Fig. 2. These reveal distinct degradation modes of the alloys investigated. For the WE-type alloy (Fig. 2a, b), localized pitting was the main mode of degradation at the early stage of the static immersion tests. With testing time passing on, discrete spots on the surface developed further, resulting in a slightly porous surface morphology (Fig. 2b). Toward week 21, an increasing number of drop-off particles were detached from the sample bulk (Fig. 2c). The ZK60 alloy showed a degradation mode similar to the WE-type alloy, but the degradation rate was significantly higher. Selective attack of the immersion solution on the magnesium matrix led to rapid material dissolution, thus resulting in an increased degradation rate and a highly porous surface morphology (Fig. 2d). Further chemical attack led to the disintegration of the sample (Fig. 2e). However, the ZK30 alloy showed a completely different mode of degradation. Throughout the immersion testing period of 21 weeks, shallow pitting damage was uniform on the sample surface (Fig. 2h). Pits developed very slowly with time (Fig. 2f, g). Few drop-off particles detached from the sample bulk were found in the immersion solution after 21 weeks, indicating that the material was able to retain its shape and structural integrity for at least 5 months.

Figure 3 compares the samples in hydrogen evolution during the static immersion tests. As can be seen, ZK60 showed quick and strong hydrogen evolution, corresponding to its degradation behavior, as shown in Fig. 1. For the WE-type alloy, however, at the early stage of immersion testing, the hydrogen evolution rate was very low and started to rise slightly after 16 weeks (112 days). Compared with ZK60 and the WE-type alloy, ZK30 showed markedly different behavior; hydrogen evolution remained

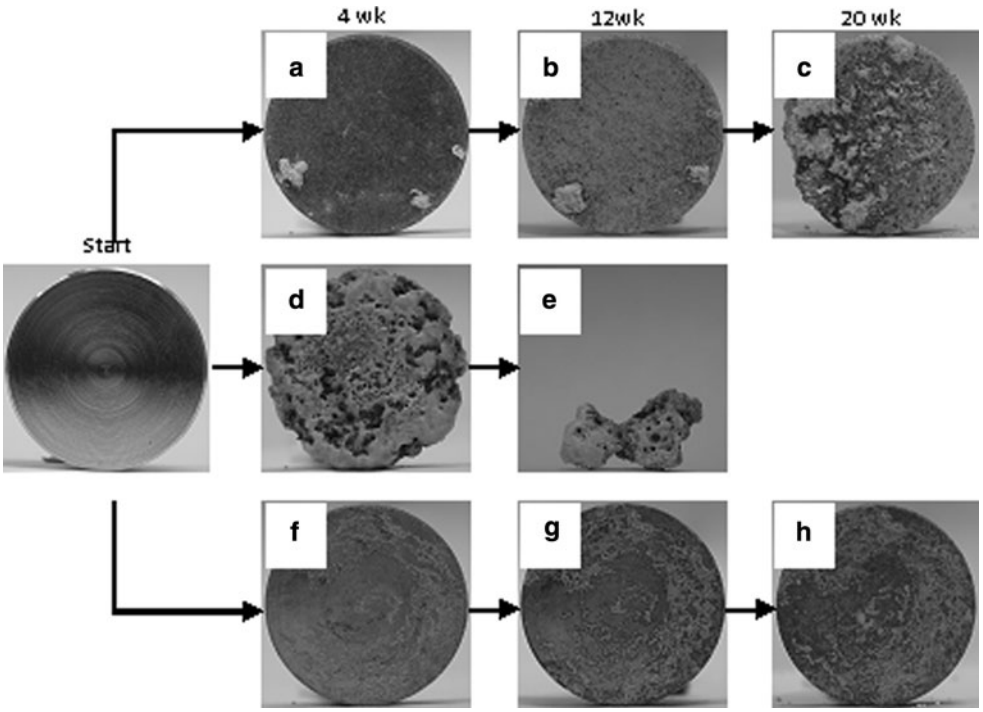

Fig. 2 Surface macro-morphologies of **a**, **b** and **c** WE-type alloy, **d** and **e** ZK60 and **f**, **g** and **h** ZK30 samples after static immersion in Hank's solution for different periods of time. ZK60 sample was completely degraded after immersion for 12 weeks

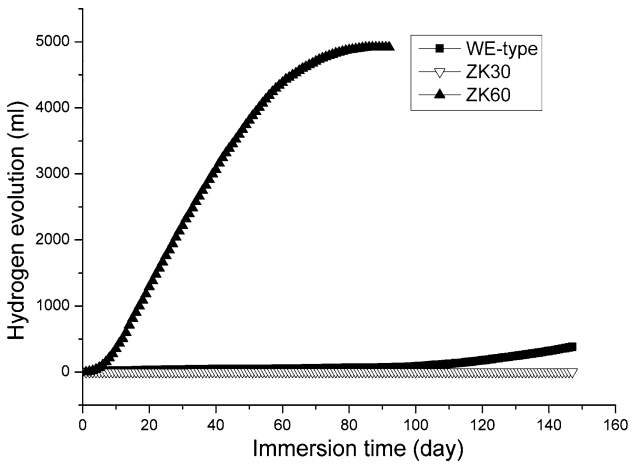

Fig. 3 Hydrogen evolution of magnesium alloy samples as a function of time during static immersion in Hank's solution

at a negligibly low level throughout the testing period of 21 weeks.

3.2 Microstructure and composition of the surface layer formed during non-static immersion

Figure 4 shows the surface morphologies of ZK30, ZK60 and WE-type alloy samples after non-static immersion in Hank's solution for 24 h. For ZK30 sample, after immersion, slight shallow pitting damage was uniformly distributed on the surface (Fig. 4a), and the pitting layer appeared to be composed of small, agglomerated particles (Fig. 4b). ZK60 sample showed a degradation pattern similar to ZK30, but the pitting damage was much severer than that on ZK30 sample (Fig. 4c, d). WE-type alloy sample showed a different mode of degradation as compared with ZK30 and ZK60 samples; pitting on the surface was highly localized (Fig. 4e) and deep into the sample bulk (Fig. 4f).

After a prolonged immersion period (7 days), the surfaces of all alloy samples were covered by a layer containing small, white particles (Fig. 5). When the surface morphologies of ZK30 (Fig. 5a, b) and WE-type alloy (Fig. 5e, f) samples after 7-day immersion were compared, it was found that more particles were formed on the WE-type alloy sample surface. It is of interest to note that the surface of ZK60 sample was completely different, being porous and sponge-like (Fig. 5c). Observation at a higher magnification showed that the surface was composed of small, agglomerated particles (Fig. 5d).

To determine the elemental compositions of the particles formed on ZK30 sample surface during the non-static immersion testing, EDX analysis was performed, which revealed the presence of Ca, Mg, P and O (Fig. 6), suggesting that these particles were mainly composed of magnesium, calcium and phosphate. The Ca/P molar ratio of the surface layer was lower than the ideal Ca/P molar ratio of hydroxyapatite (1.67). Previous studies on other magnesium

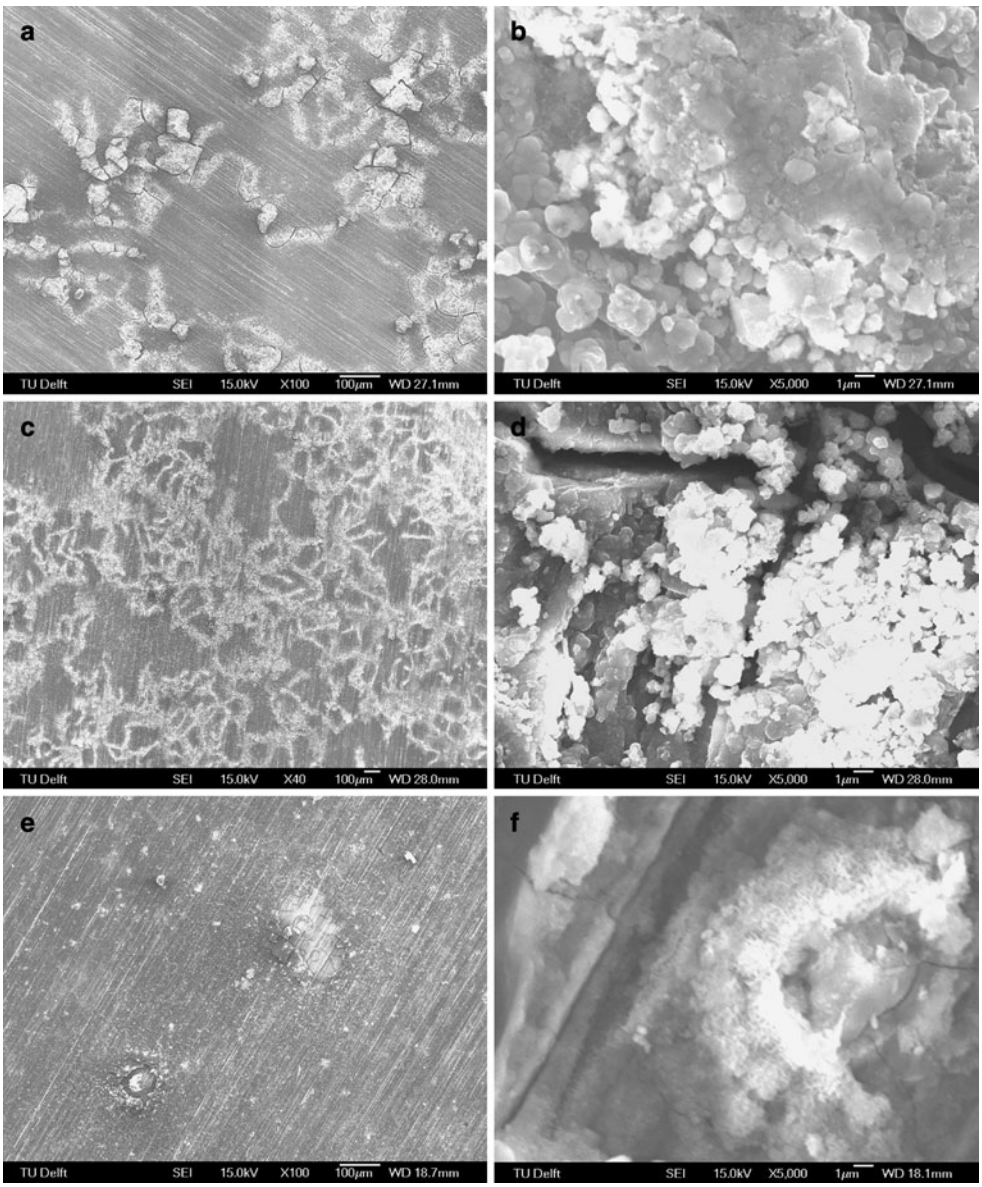

Fig. 4 SEM micrographs of **a** and **b** ZK30, **c** and **d** ZK60 and **e** and **f** WE-type alloy samples after non-static immersion in Hank's solution for 24 h

alloys for biodegradable implants showed that the surface layer was composed of magnesium calcium phosphate (Mg–CP) or amorphous calcium phosphate particles [6, 30]. It is most likely that the Mg–CP compound was also formed on the surface of ZK30 sample. In addition, it was noticed that the elemental composition of the deposited particles changed with immersion time. With increased soaking time, the atomic content of Mg decreased, while the atomic contents of Ca and P increased, as shown in Fig. 6.

To identify the phases formed on the surface of ZK30 sample after 7-day immersion, XRD analysis was carried out and the results showed strong magnesium peaks and a number of additional weak peaks (Fig. 7). The peaks emerging from the surface of the tested sample corresponded to magnesium-substitute calcium phosphate [31], which was in agreement with the finding from the EDX analysis.

3.3 Ion release during non-static immersion

The changes of ion concentrations and pH value of the soaking medium over time during non-static immersion are presented in Fig. 8. ICP-OES analysis showed that the variations of ion concentrations in the immersion medium for ZK30 were quite similar to those for the WE-type alloy. A significant increase in Mg^{2+} concentration (Fig. 8a) and

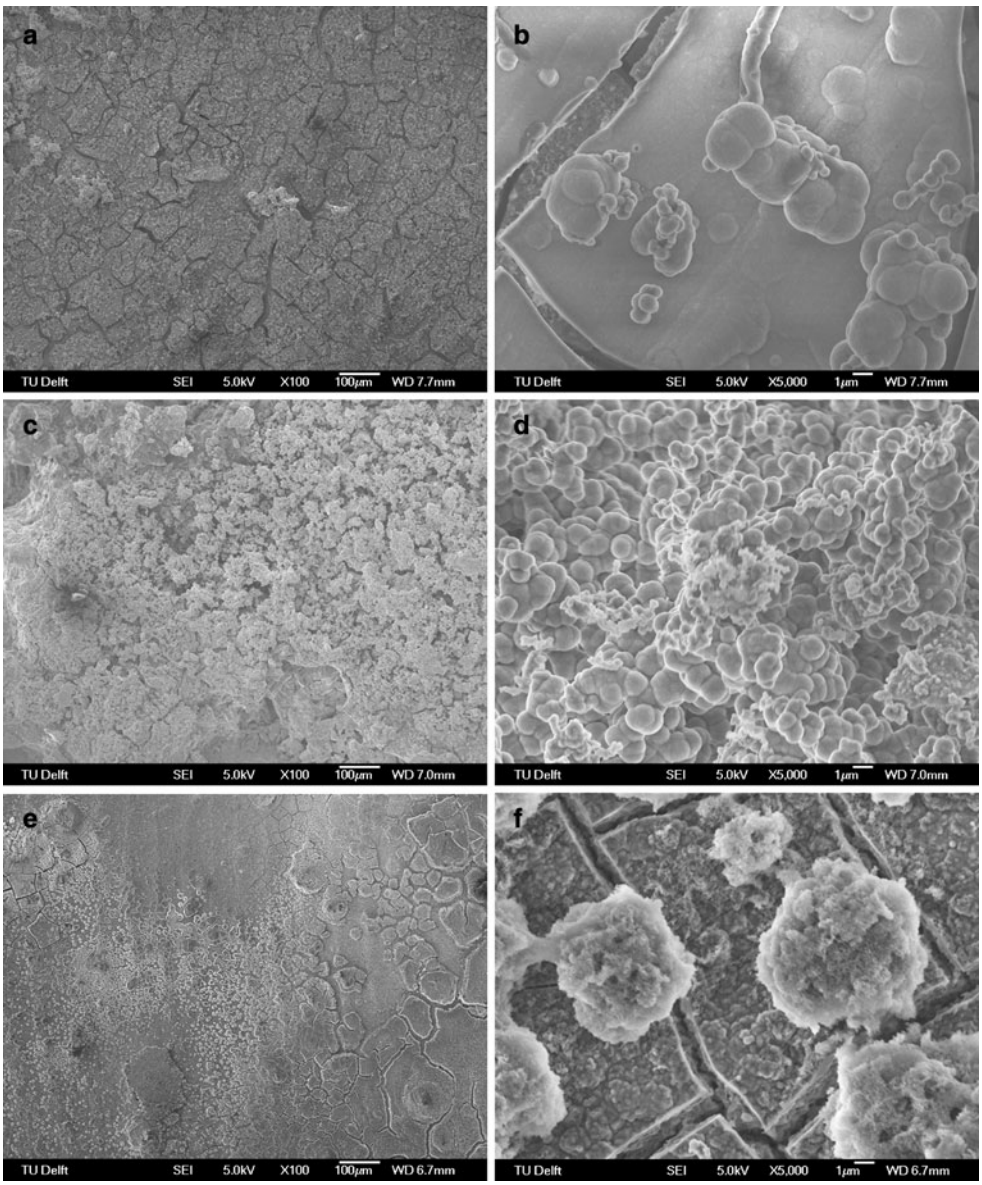

Fig. 5 SEM micrographs of **a** and **b** ZK30, **c** and **d** ZK60 and **e** and **f** WE-type alloy samples after non-static immersion in Hank's solution for 7 days

decreases in Ca^{2+} and PO_4^{3-} concentrations (Fig. 8b, c) were observed at the early stage of the immersion testing, indicating rapid release of magnesium ions and consumption of Ca^{2+} and PO_4^{3-} ions. After 1-day immersion, the Mg ion concentration tended to stabilize and the concentrations of Ca and P ions gradually changed toward those in the initial Hank's solution, as a result of refreshing 50% of the solution and the formation of a surface layer that could hinder further Mg ion release from the substrate, and Ca and P ion deposition [30, 31]. Rapid degradation of ZK60 sample, relative to ZK30 and WE-type alloy samples, resulted in a significant increase in Mg^{2+} concentration and decreases in Ca^{2+} and PO_4^{3-} concentrations in the immersion medium during the testing (Fig. 8a–c). After 1-day immersion and refreshing of 50% of the solution, the ion concentrations became quite stable and deviated much from the initial ion concentrations in Hank's solution. These results are in agreement with the degradation rate of ZK60 in the static immersion tests; all the results point towards ZK60 as the fastest degrading alloy. The results from ICP-OES analysis suggested that, during the testing, the Mg, Ca and P ion concentrations in the immersion medium for ZK30 sample were within the tolerable ranges for bone-related cells [7, 32, 33]. The Zn and Zr ion

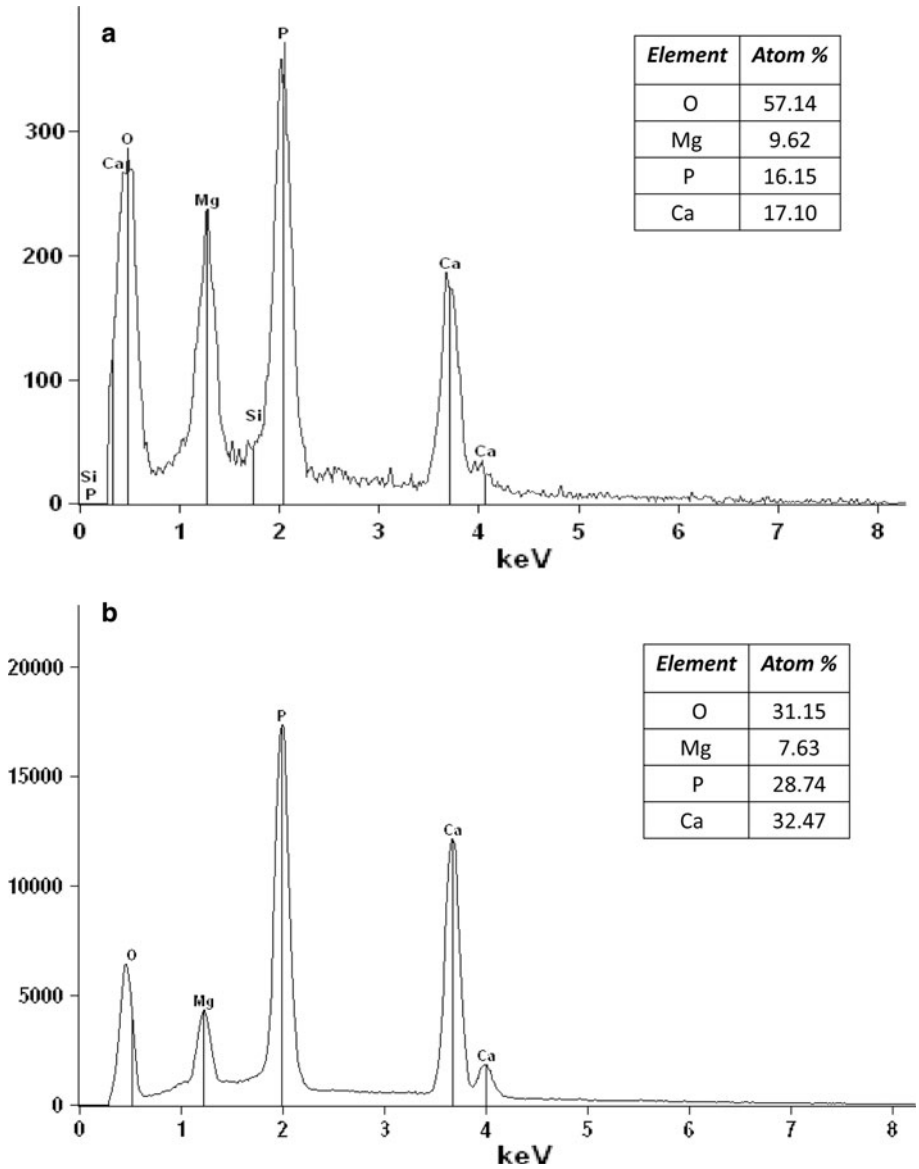

Fig. 6 EDX analysis of the particles deposited on the surfaces of ZK30 alloy samples after non-static immersion in Hank's solution for **a** 24 h and **b** 7 days

concentrations in the immersion medium were below 0.0001 mmol/l, indicating limited release of these two elements to the immersion medium.

The variation of the pH value of the immersion medium with time was determined and the results are shown in Fig. 8d. The pH value of the solution with ZK30 sample increased from 7.30 to 8.31 during the first 3 days. Refreshing 50% of the solution did not seem to affect the tendency. Thereafter, the pH value decreased slightly to 7.95 on day 5 and remained stable at the level of 8.0 during the last 3 days. The trend of the pH change of the solution with WE-type alloy sample was very similar to that with ZK30 sample, although the pH values were all higher. However, the pH value of the solution with ZK60 sample changed in a different way; the pH value increased rapidly to 10.31 during the first day immersion and then gently increased to 10.65 on day 7.

3.4 Cytotoxicity of ZK30 in comparison with the WE-type alloy and HA

Since ZK60 showed a rather high degradation rate that was not desirable for biomedical applications, cytotoxicity evaluation of ZK60 was not made. The results obtained from ICP-OES analysis and pH measurements suggested that the degradation eluates from the ZK30 and WE-type alloy might not induce toxicity to bone-related cells. To confirm this hypothesis, cytotoxicity tests were performed and biocompatible HA was used as reference. It was found that, at the tested concentration of the

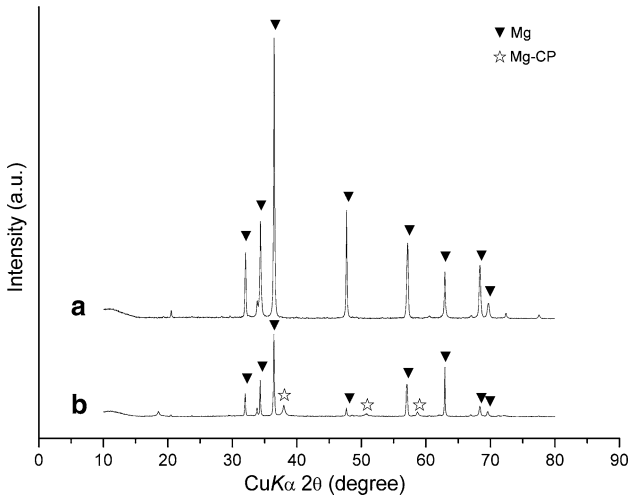

Fig. 7 XRD patterns of ZK30 samples **a** before and **b** after non-static immersion in Hank's solution for 7 days

extract, ZK30 and WE-type alloy samples displayed cytocompatibilities quite similar to HA after 1-day incubation (Fig. 9). After a prolonged incubation period of 7 days, the rBMSC cell proliferation in the extract of ZK30 sample was found to be significantly higher than that of HA sample ($P < 0.05$) and slightly higher than that of WE-type alloy sample.

4 Discussion

In recent years, extensive research on magnesium and its alloys as potential biodegradable materials has been carried out. However, only limited efforts have been made to study the alloys with compositions pertaining to biomedical applications. In the present research, the general long-term degradation behavior of the WE-type alloy, ZK30 and ZK60 alloys was evaluated by static immersion tests in which the concentration of Cl^- ions was maintained at a constant level. Such a static immersion system may not exactly simulate the actual physiological conditions in the human body, because the body fluid circulates dynamically and, moreover, ion concentrations differ in different parts of the human body [21]. Nevertheless, since the local concentration of Cl^- ions is one of the most important factors that determines the degradation rate of magnesium alloys when they are exposed to an aggressive electrolyte such as simulated body fluid or a NaCl solution [11], different behavior between different magnesium alloys in degradation rate can be revealed, if testing parameters such as ion concentrations in the immersion system are kept unchanged.

For magnesium alloys to be used as viable implant materials, their degradation rates should not exceed the healing rate of the affected tissue. They should remain present in the body and maintain their mechanical integrity

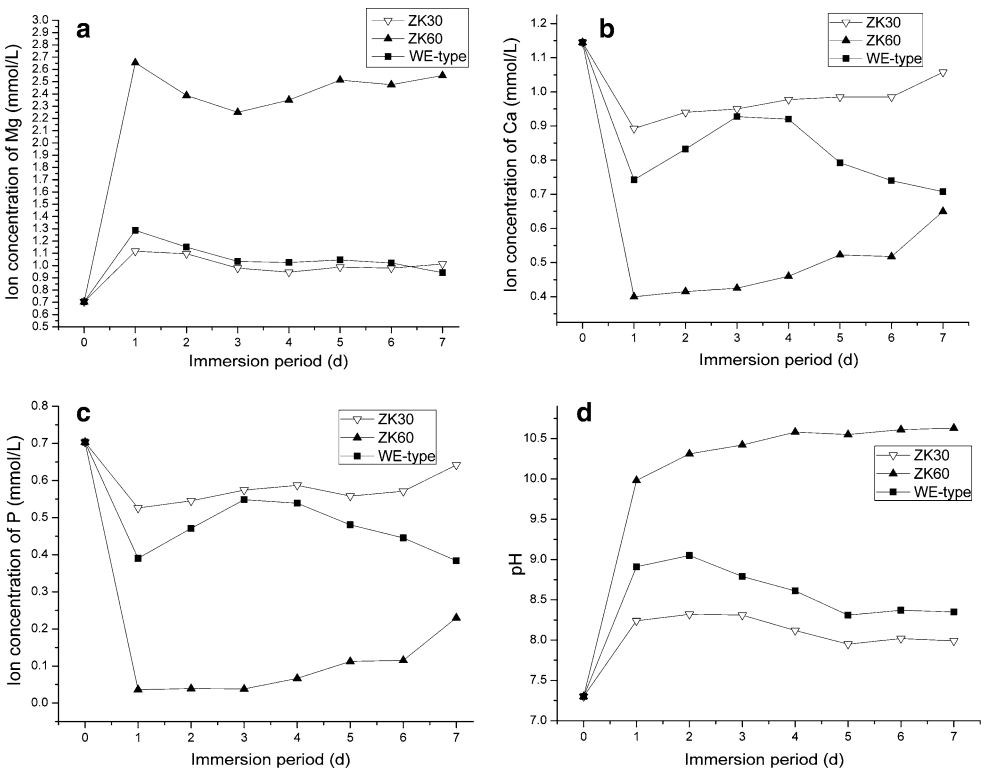

Fig. 8 Variations of **a** Mg, **b** Ca and **c** P ion concentrations and **d** pH value of the medium with time during non-static immersion in Hank's solution. Zn and Zr iron concentrations were below 0.0001 mmol/l and therefore they are not presented

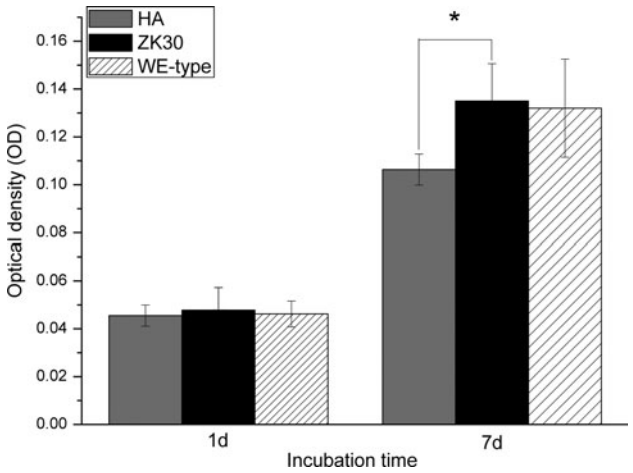

Fig. 9 Rabbit marrow stromal cell viability expressed by the optical density of the cells measured with enzyme-linked immunoadsorbent assay after one and 7 days of culture in ZK30, WE-type alloy and HA extraction media. The asterisk (*) indicates that the cell proliferation in the ZK30 alloy extract was significantly different from that of the HA extract ($P < 0.05$)

at least for a period of 12–18 weeks, while the bone tissue heals itself [1, 6]. The results obtained from previous in vivo studies have shown a moderate degradation rate of WE43 [6]. The results from the present long-term static immersion tests showed that the ZK30 alloy possessed a higher corrosion resistance than the WE-type alloy. The superior corrosion resistance of ZK30 may be attributed to the beneficial effects of certain amounts of Zn and Zr on the corrosion resistance by overcoming the harmful corrosive effect of impurities and leading to finer grain sizes [11, 15–17] and to the precipitation of phosphate that forms a protective layer on the surface. By contrast, ZK60 showed a rather accelerated degradation rate; by the end of week 12, the sample was degraded completely. Obviously, the significant difference between ZK30 and ZK60 in degradation behavior is related to the higher content of zinc in the latter leading to the formation of second-phase particles and micro-galvanic cells. It has been reported that, the addition of zinc to magnesium is usually limited to 1–3%, if improvement in corrosion resistance is expected [34, 35]. Within the range of 1–3%% Zn, an increase of Zn content from 2 to 3% moves the corrosion potential to a more negative value and thus reduces the corrosion resistance [36]. When the Zn content in a magnesium alloy goes beyond 3 wt%, a considerable amount of the Mg_7Zn_3 phase will form in the magnesium matrix according to the Mg–Zn binary phase diagram [12], and these second-phase particles will result in micro-galvanic coupling with the matrix, thus accelerating the corrosion of the material [36]. The results suggest that the degradation rate of Zn-containing magnesium alloys produced by the conventional techniques may be adjustable by fine-tuning the Zn content to meet the clinical needs of implant materials in degradation rate for different applications.

It is worth mentioning that for wrought Mg–Zn–Zr alloys produced through the conventional casting and forming routes (i.e. those in the ASTM standards), the zinc content is usually limited to the maximum solubility of zinc in magnesium (6.2 wt% at 635°C) so as to make alloy responsive to the solution and aging treatment and to avoid the formation of the Mg + MgZn eutectic in the alloy. A zinc content closer to this maximum solubility leads to more MgZn precipitates at room temperature under the equilibrium condition and thus to higher mechanical strength but lower corrosion resistance. However, when rapid solidification techniques are employed, such as melt spinning or copper-mould casting, the Zn content can be extended far beyond the maximum solubility of 6.2 wt% under the equilibrium condition. Within the glass-forming composition range of 21–35 at.% zinc, corresponding to 42–59 wt% zinc, the amorphous structure of the parent liquid can be retained in the rods with a diameter of 1 mm or larger [37]. When the zinc content is over 28 at.% (or 51 wt%), a dense amorphous layer rich in Zn (instead of Mg) and oxygen is formed to protect the surface, slow down degradation rate and reduce hydrogen evolution per unit time [37, 38]. This concerns a different, yet very interesting strategy in alloy design and material fabrication for biodegradable magnesium alloys.

The degradation of magnesium alloys inevitably leads to the evolution of hydrogen. Hydrogen evolving from a degrading magnesium implant can be accumulated in gas pockets next to the implant, which will delay the healing of the surgery region and lead to necrosis of tissues, because the gas pockets can cause tissues and tissue layers to separate [39]. Therefore, it is of vital importance to limit the hydrogen evolution from magnesium implant to a minimum level. Obviously, the most efficient and direct way to lowering the hydrogen evolution is to improve the corrosion resistance of the magnesium alloy. Compared with the WE-type alloy, ZK30 had noticeably less release of hydrogen over the first 17 weeks and a negligibly low level of hydrogen evolution was retained over a period from the 17th week to the 21st week. This is attributed to the superior corrosion resistance of the alloy, because every dissolved mole of magnesium produces 1 mol of hydrogen [11].

$$Mg(s) + 2H_2O \rightarrow Mg(OH)_2(s) + H_2(g) \quad (1)$$

In a previous in vivo study, hydrogen evolving from WE43 during degradation was considered tolerable and could be dispersed by surrounding tissues [6]. It is therefore reasonable to expect that the hydrogen evolution from ZK30 during degradation should be a matter of less concern after

implantation, because the amount of hydrogen release from ZK30 is less than that from the WE-type alloy.

The surface characteristics of magnesium alloys relevant to biomedical applications, such as surface layer deposition, ion release and alkanization caused by in vivo corrosion, are another concern in selecting these alloys as biodegradable materials. The results obtained from SEM, EDX and XRD analyses confirmed that the main compound of the surface layer on ZK30 sample was Mg^{2+} substituted calcium phosphate, which was formed by the dissolution of magnesium and simultaneously deposition of calcium phosphate from Hank's solution. Such a layer is believed to bring additional benefits to the material at the early stage after implantation, since it has shown improved biocompatibility and osteoconductivity in comparison with calcium phosphate and hydroxyapatite [40, 41]. It was reported that magnesium alloys could bond with surrounding tissue by the formation of a Mg-substituted calcium phosphate layer on the surface. Osteoconductive bioactivity of magnesium-based metals was suggested, based on the observed increase in bone apposition around magnesium-based implants as compared to polylactic acid (PLA) [6]. It should however be noted that the surface layer formed on magnesium alloys is not as dense and homogeneous as a layer formed by applying coating for the improvement of corrosion resistance [42]. Therefore, the alloying elements and their amounts are the important factors that contribute to the enhanced corrosion resistance of ZK30. It is reasonable to expect that ZK30, being able to promote the precipitation of a magnesium-substituted calcium phosphate layer, will possess enhanced osteoconductivity as WE43 does [6].

It should be kept in mind that, even though the surface layer formed on ZK30 sample is expected to be biocompatible and osteoconductive as that formed on the surface of other magnesium alloys, it is necessary to determine the ion release and pH values during non-static immersion, because the release of metallic ions and alkanization during the corrosion of Mg-based alloys may indicate cytotoxicity to surrounding tissues. Therefore, the ion concentrations of Mg and alloying elements in the immersion media for ZK30 and WE-type alloy samples were determined. The results confirmed that the Mg, Zn and Zr ion concentrations in the non-static immersion medium for ZK30 throughout the testing period of 7 days were all below tolerable levels for bone-related cells [43, 44]. The consumption of Ca^{2+} and PO_4^{3-} ions was attributed to the deposition of magnesium calcium phosphate on sample surface, which is important for the formation of bonding between material and bone tissue. As far as the pH variation is concerned, it is known that cells are highly sensitive to environment fluctuations, and a significant increase in pH value can cause fatal effects on the viability of cell and serious hemolysis. The results of the present research indicate that the degradation of ZK30 caused more moderate changes in pH value (around 8.0) than that of the WE-type alloy, and the pH values fluctuating slightly over time fell into the tolerable range of pH values for most human cells (6.0–9.0) [45]. One may therefore expect that the degradation process of the ZK30 alloy will not cause significant environment fluctuations that may be fatal for cells and the alloy will possess a cytocompatibility similar to or better than the WE43 alloy. To confirm this hypothesis, a preliminary in vitro cell-material interaction analysis based on the extracts formed by the degradation of samples in a cell culture medium was performed. As compared to HA, both the ZK30 and WE-type alloy did not show significant cytotoxicity against the rBMSC cells in the tested concentration of the extract. Considering the fact that HA with a chemical composition similar to that of the natural bone is biocompatible with the hard tissue of the human being, it is reasonable to envisage that the ZK30 alloy is cytocompatible to the surrounding tissues after implantation. Moreover, it was observed that, after 7-day incubation, the ionic products of ZK30 dissolution could provide a better stimulus for cell proliferation than those of HA and the WE-type alloy ($P < 0.05$). The enhanced cell proliferation could be attributed to the moderate Mg ion release from ZK30, which may have a beneficial effect on some structures including those of the cells in the relevant local tissue, in addition to the favorable characteristics including the variation of pH value in the immersion solution with time and surface magnesium calcium phosphate deposition [46]. Zreiqat et al. [47] reported that magnesium ion modified bioceramic substrata could enhance the human bone-derived cell (HBDC), and due to functional roles and presence in bone tissue, magnesium may actually have stimulatory effects on the growth of new bone tissue [1, 48]. It may thus be inferred that the enhancement in cell proliferation in the presence of the ZK30 magnesium alloy may result in enhanced bone healing in vivo. However, further in vitro cell-culture tests and the characterization of in vitro degradation behavior of the material in the presence of bone cells are necessary. In addition, in vivo studies will be needed to validate and supplement the in vitro results. Encouraging in vivo results of ZK30 are expected. This expectation is based on the positive results of the in vivo tests of the single-phase binary Mg–6Zn alloy without MgZn precipitates after a solid solution treatment and extrusion [49], being similar to the present ZK30 alloy in terms of phase constitution. The in vivo tests of this binary Mg–6Zn alloy indicated (i) a relatively high degradation rate of the alloy after 14 weeks of implantation (2.32 mm/year) in comparison with other magnesium alloys, (ii) different surface morphologies and compositions between in vitro and in vivo, (iii) formation of

trabeculae and osteoblasts despite a gap between the implant and surrounding bone tissues due to rapid degradation, and (iv) good biocompatibility as evidenced by no negative effect of zinc release on the heart, kidney, liver and spleen [49]. In addition, the same binary alloy Mg–6Zn without the specific heat treatment, presumably containing MgZn precipitates, subjected to animal tests for 14 weeks, also showed no effect on the chromatics, structure or function of heart, liver, kidney or spleen after implantation for 6 weeks [50].

5 Conclusions

In the present in vitro study, magnesium alloys with zinc and zirconium as the alloying elements (ZK30 and ZK60) were investigated with respect to (i) their degradation rate and hydrogen evolution during static immersion, (ii) ion release and the surface layer formed during non-static immersion and (iii) cytocompatibility with the rBMSC cells in order to exploit their potential as biodegradable materials. Comparison was made with a WE-type magnesium alloy. Among these three magnesium alloys, the ZK30 alloy showed the lowest degradation rate and the least hydrogen evolution during static immersion over a period of 21 weeks. It is likely that the degradation rate of Mg–Zn–Zr alloys can be adjusted by modifying the Zn content in the alloy. Furthermore, ZK30 showed moderate ion release, surface alkanization and, more importantly, good cytocompatiblily with a potential stimulatory effect on bone-related cells. The results obtained from these investigations suggested that Zn- and Zr-containing magnesium alloys, especially ZK30, could hold promise as candidate materials with adjustable degradation rate for orthopedic applications.

Acknowledgements The authors would like to thank Prof. Jiang Chang and Dr. Wanyin Zhai of the Biomaterials and Tissue Engineering Research Center, Shanghai Institute of Ceramics, Chinese Academy of Sciences, China, for the preparation of hydroxyapatite disks, assistance in the cytotoxicity tests and fruitful discussions.

References

1. Staiger MP, Pietak AM, Huadmai J, Dias G. Magnesium and its alloy as orthopaedic biomaterials: a review. Biomater. 2006;27:1728–34.
2. Wintermantel EHS. Medizintechnik mit Biokompatiblen Werkstoffen und Verfahren. 3rd ed. Berlin, Heldelberg, New York: Springer; 2002.
3. Song G. Control of biodegradation of biocompatible magnesium alloys. Corros Sci. 2007;49:1696–701.
4. Witte F, Hort N, Vogt C, Cohen S, Kainer KU, Willumeit R, Feyerabend F. Degradable biomaterials based on magnesium corrosion. Curr Opin Solid State Mater Sci. 2008;12:63–72.
5. El-Rahman SSA. Neuropathology of aluminium toxicity in rats (Glutamate and GABA impairment). Pharmacol Res. 2003; 47:189–94.
6. Witte F, Kaese V, Haferkamp H, Switzer E, Meyer-Lindenberg A. In vivo corrosion of four magnesium alloys and the associated bone response. Biomater. 2005;24:4913–20.
7. Gu X, Zheng Y, Cheng Y, Zhong S, Xi T. In vitro corrosion and biocompatibility of binary magnesium alloys. Biomater. 2009; 30:484–98.
8. Schranz D, Zartner P, Michel-Behnke I, Akinturk H. Bioresorbable metal stents for percutaneous treatment of critical recoarctation of the aorta in a newborn. Catheter Cardiovasc Interv. 2006;67:671–3.
9. Ahmed T, Rack HJ. Low modulus biocompatible titanium base alloys for medical devices. US Patent, No. 5871595.
10. Boehlert CJ, Knittel K. The microstructure, tensile properties, and creep behaviour of Mg–Zn alloys containing 0–4.4 wt% Zn. Mater Sci Eng A. 2006;417:315–21.
11. Song G, Atrens A. Corrosion mechanisms of magnesium alloys. Adv Eng Mater. 1999;1:11–33.
12. Friedrich HE, Mordike BL. Magnesium technology. Berlin, Heidelburg: Springer-Verlag; 2006.
13. Gao JC, Wu S, Qiao LY, Wang Y. Corrosion behavior of Mg and Mg-Zn alloys in simulated body fluid. Trans Nonferrous Met Soc China. 2008;18:588–92.
14. Seiler H. Metal ions in biological system. In: Concepts on metal ion toxicity. vol. 20. Marcel Dekker, Inc. 1986.
15. Babkin VM. Effect of zirconium on the grain size of magnesium containing 4.5% Zn. Met Sci Heat Treat. 2004;5:543–4.
16. Song G, St John D. The effect of zirconium grain refinement on the corrosion behavior of magnesium-rare earth alloy MEZ. J Light Met. 2002;1:1–16.
17. Song G. Recent progress in corrosion and protection of magnesium alloys. Adv Eng Mater. 2005;7:563–86.
18. Saldana L, Mendez-Vilas A, Jiang L, Multigner M, Conzalez-Carrasco JL, Perez-Prado MT. In vitro biocompatibility of an ultrafine grained zirconium. Biomater. 2007;28:4343–54.
19. Kulakov OB, Doktorov AA, D'iakova SV, Denisov-Nikol'skii I, Grotz KA. Experimental study of osseointegration of zirconium and titanium dental implants. Morfologiia. 2005;127:52–5.
20. Loos A, Rohde R, Haverich A, Barlach S. In vitro and in vivo biocompatibility testing of absorbable metal stents. Macromol Symp. 2007;253:103–8.
21. Levesque J, Hermawan H, Dube D, Mantovani D. Design of a pseudo-physiological test bench specific to the development of biodegradable metallic biomaterials. Acta Biomater. 2008;4:284–95.
22. Marc B, Lemaitre J. Can bioactivity be tested in vitro with SBF solution? Biomaterials. 2009;30:2175–9.
23. Yamamoto A, Hiromoto S. Effect of inorganic salts, amino acids and proteins on the degradation of pure magnesium in vitro. Mater Sci Eng C. 2009;29:1559–68.
24. Kokubo T. Surface chemistry of bioactive glass-ceramics. J Non-Cryst Solids. 1990;120:138–51.
25. Mauney JR, Jaquiery C, Volloch V, Heberer M, Martin I, Kaplan DL. In vitro and in vivo evaluation of differentially demineralized cancellous bone scaffolds combined with human bone marrow stromal cells for tissue engineering. Biomater. 2005;26:3173–85.
26. Cory AH, Owen TC, Barltrop JA, Cory JG. Use of an aqueous soluble tetrazolium/formazan assay for cell growth assays in culture. Cancer Commun. 1991;3:207–12.

27. Li Z, Gu X, Lou S, Zheng Y. The development of binary Mg-Ca alloys for use as biodegradable materials within bone. Biomater. 2008;29:1329–44.
28. Jarcho M. Calcium phosphate ceramics as hard tissue prosthetics. Clin Orthop Relat Res. 1981;157:259–78.
29. Neo M, Kotani S, Nakamura T, Yamamuro T, Ohtsuki C, Kokubo T, Bando Y. A comparative study of ultra structure of the interfaces between four kinds of surface-active ceramics and bone. J Biomed Mater Res. 1992;26:1419–32.
30. Xu L, Zhang E, Yin D, Zeng S, Yang K. In vitro corrosion behavior of Mg alloys in a phosphate buffered solution for bone implant application. J Mater Sci Mater Med. 2008;19:1017–25.
31. Yang L, Zhang E. Biocorrosion behavior of magnesium alloy in different simulated fluids for biomedical application. Mater Sci Eng C. 2009;29:1691–6.
32. Romani A, Scarpa A. Regulation of cell magnesium. Arch Biochem Biophys. 1992;298:1–12.
33. Ilich JZ, Kerstetter JE. Nutrition in bone health revisited: a story beyond calcium. J Am Coll Nutr. 2000;19:715–37.
34. Bhan S, Lal A. The Mg–Zn–Zr system. J Phase Equil. 1993; 14:634–7.
35. Froats A, Aune TK, Hawke D, Unsworth W, Hillis J. ASM handbook: corrosion. vol. 1, 39 edn. ASM Inter. 1987; p. 740–54.
36. Zhang E, Yin D, Xu L, Yang L, Yang K. Microstructure, mechanical and corrosion properties and biocompatibility of Mg-Zn-Mn alloys for biomedical application. Mat Sci Eng C. 2009;29:987–93.
37. Ma E, Xu J. Biodegradable alloys: the glass window of opportunities. Nat Mater. 2009;8:855–7.
38. Zberg B, Uggowitzer PJ, Löffler J. ZMgZnCa glasses without clinically observable hydrogen evolution for biodegradable implants. Nat Mater. 2009;8:887–91.
39. Mcbride ED. Absorbable metal in bone surgery. J Am Med Assoc. 1938;111:2464–7.
40. Qi G, Zhang S, Khor KA, Lye SW, Zeng X, Weng W, Liu C, Venkatraman SS, Ma L. Osteoblastic cell response on magnesium-incorporated apatite coatings. Appl Surf Sci. 2008;255:304–7.
41. Sader M, LeGeros R, Soares G. Human osteoblasts adhesion and proliferation on magnesium-substituted tricalcium phosphate dense tablets. J Mater Sci Mater Med. 2009;20:521–7.
42. Retting R, Virtanen S. Composition of corrosion layers on a magnesium rare-earth alloy in simulated body fluids. J Biomed Mater Res A. 2009;88A:359–69.
43. Hallab NJ, Vermes C, Messina C, Roebuck KA, Glant TT, Jocobs JJ. Concentration- and composition-dependent effects of metal ions on human MG-63 osteoblasts. J Biomed Mater Res. 2002;60:420–33.
44. Schmalz G, Langer H, Schweikl H. Cytotoxicity of dental alloy extracts and corresponding metal salt solution. J Dent Res. 1998;77:1772–8.
45. Harrison MA, Rae IF. General techniques of cell culture. Cambridge: Cambridge University Press; 1997. p. 7–31.
46. William D. New interests in magnesium. Med Dev Tech. 2006;17:9–10.
47. Zreiqat H, Howlett CR, Zannettino A, Evans P, Schulze-Tanzil G, Kanbe C. Mechanisms of magnesium-stimulated adhesion of osteoblastic cells to commonly used orthopedic implants. J Biomed Mater Res. 2002;62:175–84.
48. Yamasaki Y, Yoshida Y, Okazaki M, Shimazu A, Kubo T, Akagawa Y, Uchida T. Action of FGMgCO_3Ap-collagen composite in promoting bone formation. Biomater. 2003;24:4913–20.
49. Zhang S, Zhang X, Zhao C, Li J, Song Y, Xie C, Tao H, Zhang Y, He Y, Jiang Y, Bian Y. Research on an Mg-Zn alloy as a degradable biomaterial. Acta Biomater. 2010;6:626–40.
50. He YH, Tao HR, Zhang Y, Jiang Y, Zhang SX, Zhao CL, Li JN, Zhang BL, Song Y, Zhang XN. Biocompatibility of bio-Mg–Zn alloy within bone with heart, liver, kidney and spleen. Chin Sci Bull. 2009;54:481–91.